# Supporting Information

## Boosting High Stability on $BiVO_4$ Photoanodes: In-situ Cocatalyst Passivation and Immobilization by Functional Fluorine Anions

*Rui-Ting Gao,[a] Lijun Wu,[a] Shujie Liu,[a] Kan Hu,[a] Xianhu Liu,[b] Jun Zhang,*[a] and Lei Wang*[a]*

*[a] School of Chemistry and Chemical Engineering & Inner Mongolia Engineering and Technology Research Center for Catalytic Conversion and Utilization of Carbon Resource Molecules, Inner Mongolia University, 235 West University Street, Hohhot 010021, China*

*[b] Key Laboratory of Materials Processing and Mold, Ministry of Education, Zhengzhou University, Zhengzhou 450002, China*

** Corresponding authors: cejzhang@imu.edu.cn (J.Z.); wanglei@imu.edu.cn (L.W.)*

## Methods

### *1. Material preparation*

BiOI was prepared according to previous reported method.[1] 100 ml KI (0.4 M) was added into 0.04 M $Bi(NO_3)_3 \cdot 5H_2O$, in which $HNO_3$ was added to adjust the pH value of 1.7. This solution was mixed with a 40 ml ethanol solution containing 0.23 M p-benzoquinone. The anode deposition was performed at -0.1 $V_{Ag/AgCl}$ for 300 s to form BiOI. The dimethyl sulfoxide (DMSO) solution containing 0.2 M vanadyl acetylacetonate ($VO(acac)_2$) was dropped on the BiOI for annealing at 450 °C for 2 h. The annealed $BiVO_4$ was slowly stirred in 1 M NaOH for 30 minutes to remove excess $V_2O_5$. The as-prepared $BiVO_4$ is noted as BVO in the manuscript.

For the preparation of $Co(CO_3)_xOH_y/BiVO_4$, the precursor solution containing 6 mM $Co(NO_3)_2 \cdot 6H_2O$ and 30 mM urea was thoroughly stirred. The $BiVO_4$ was put into the stainless steel reactor (50 mL) with a 30 mL precursor solution for reaction at 120 °C for 6 h. The preparation of $F:Co(CO_3)_xOH_y/BiVO_4$ is similar to that of $Co(CO_3)_xOH_y/BiVO_4$, only 4.7 mM ammonium fluoride ($NH_4F$) was added in precursor containing $Co(NO_3)_2 \cdot 6H_2O$ and urea.

For the preparation of $Co_3O_4$ and $F:Co_3O_4$. The precursor was prepared with 1.2 mM $Co(NO_3)_2 \cdot 6H_2O$, 8.4 mM urea, and 0.4 mM $SnCl_4$ in 20 mL deionized water. After being fully stirred, the $BiVO_4$ and precursor were put into the reactor for reaction at 120 °C for various times (10, 20, 30, and 40 min). Then, the sample was heating at 400 °C for 1 h. For the $F:Co_3O_4$, the sample and 0.05 g $NH_4F$ were placed in a tube furnace for annealing at 400 °C for 1 h under Ar atmosphere. The F-treated $BiVO_4$ was soaked up-to-down in a 10 mL solution containing $NH_4F$ (1 M) for 3 h.

### *2. Photoelectrochemical measurements*

Photoelectrochemical measurements were measured in a standard three-electrode system with an electrochemical analyzer (CHI760D, CH Instruments, Inc.). The light source was simulated sunlight AM 1.5G (100 mW $cm^{-2}$, PLS-FX300HU, Beijing Perfectlight Technology Co., Ltd.). All samples were illuminated from the back sides. 1 M KBi solution with pH of 9.5 was used as the electrolyte. Photocurrent vs voltage (*J-V*) curves were recorded by scanning the potential from -0.7 to 0.6 $V_{Ag/AgCl}$ with a rate of 10 mV $s^{-1}$ under AM 1.5 G back illumination. Electrochemical impedance spectroscopy (EIS) was performed at 0.6 $V_{RHE}$ with a small AC amplitude of 10 mV in the frequency range of $10^{-2}$-$10^5$ Hz under back illumination. Mott-Schottky spectra were obtained in the voltage window of 0~0.6

$V_{RHE}$ in the dark (increment: 10 mV, frequency: 1 kHz).

During the *J-t* measurement, various amounts of F anions (1 M) were added into KBi electrolyte (15 mL) without changing pH value. For comparison, 0.5 μL $Co^{2+}$ (0.1 M $Co(NO_3)_2 \cdot 6H_2O$), 0.5 μL $Fe^{3+}$ (0.1 M $Fe(NO_3)_3 \cdot 9H_2O$), and 0.5 μL $Ni^{2+}$ (0.1 M $Ni(NO_3)_2 \cdot 6H_2O$) ions were added into KBi (15 mL). During the activation of $Co_3O_4$, 6 μL $NH_4F$ (1 M) was added into 15 ml KBi electrolyte. For the long-term stability measurement of $Co(CO_3)_xOH_y/BiVO_4$ in KBi with the additive F, 0.5 μL $NH_4F$ (1 M) was added into the fresh KBi and measured at 0.6 $V_{RHE}$ under AM 1.5G back illumination. Incident light-electron conversion efficiency (IPCE) was measured at 1.23 $V_{RHE}$ in 1 M KBi using Xe lamp (CEL-SLF-Vertex, CEAULIGHT Co., Ltd.). Use the following formula to calculate IPCE.

$$IPCE(\%) = \frac{J \times 1240}{\lambda \times p_{Light}} \times 100\% \qquad (1)$$

where $J$ presents the photocurrent density (mA $cm^{-2}$) obtained from the electrochemical workstation. $\lambda$ and $P_{light}$ are the incident light wavelength (nm) and the power density obtained at a specific wavelength (mW $cm^{-2}$), respectively. Applied bias photon-to-current efficiency (ABPE) can be calculated using the following equation:

$$ABPE(\%) = \frac{J \times (1.23 - V_b)}{p_{total}} \qquad (2)$$

$J$ is the photocurrent density (mA $cm^{-2}$) obtained from the electrochemical workstation. $V_b$ refers to the applied bias versus RHE (V), and $P_{total}$ is the total light intensity of AM 1.5 G (100 mV $cm^{-2}$). The charge separation efficiency ($\eta_{sep}$, the yield of photo-generated holes reaching the semiconductor/electrolyte interface) and the surface charge transfer efficiency ($\eta_{trans}$, the yield of holes participating in the water oxidation reaction after reaching the electrode/electrolyte interface) can be calculated using the following formula .

$$\eta_{surface} = \frac{J_{H_2O}}{J_{Na_2SO_3}} \qquad (3)$$

$$\eta_{abs \times sep} = \frac{J_{Na_2SO_3}}{7.5} \qquad (4)$$

While $J_{H_2O}$ and $J_{Na_2SO_3}$ are the photocurrent densities obtained in 1 M KBi without and with 0.2 M $Na_2SO_3$, 7.5 mA/$cm^2$ is the theoretical limit of $BiVO_4$ under AM 1.5 G illumination.

Photocurrent spectra were collected at 1.23 $V_{RHE}$ in KBi in the range of 350-550 nm using amonichromatic light by a Xe-lamp (CEL-SLF-Vertex). The gas production was collected with a (Shimadzu, GC-2014C).

### *3. Materials characterization*

The crystalline structure was identified by X-ray diffraction analysis (XRD, Rigaku RINT-2000) using Cu Kα radiation at 40 kV and 40 mA. The elemental composition was determined by X-ray photoelectron spectroscopy (XPS, ESCALAB 250xi, Thermo Fisher Scientific). The elemental contents in electrolyte was analyzed using inductively coupled plasma optical emission spectroscopy (ICP-OES-720ES, Agilent, USA). Scanning electron microscopy (SEM) and transmission electron microscopy (TEM) were carried out using FE-SEM-Supra 55 (Zeiss, Germany) and JEM-2100F (JEOL, Japan) systems. UV-visible diffuse reflectance spectra were performed on a UV-2600 (Shimadzu) spectrometer by using $BaSO_4$ as the reference.

Reference

1. T. W. Kim, K.-S. Choi. *Science* 2014, *343*, 990-994.

**Table S1.** Comparison of PEC activities and stability for cocatalysts decorated on $BiVO_4$ photoanodes.

| Photoanode | *J* (mA $cm^{-2}$ @1.23 $V_{RHE}$) | Stability | Electrolyte | Reference |
|---|---|---|---|---|
| **$Co(CO_3)_xOH_y/BiVO_4$** | **5.1**<br>**5.1** | **10 h@0.6 $V_{RHE}$**<br>**100 h@0.6 $V_{RHE}$** | **1 M KBi**<br>**1 M KBi+$F^-$** | ***This work.*** |
| $NiOOH/FeOOH/BiVO_4$ | 4.8 | 500 h@0.6 $V_{RHE}$ | 1 M KBi+$V_2O_5$ | ***Nature Energy*** 2018, 3, 53. |
| $Mo:BiVO_4/Ni/Sn$ | 2.6 @0.6 $V_{RHE}$ | 1100 h@0.6 $V_{RHE}$ | 1 M KBi+$Fe^{2+}$ | ***Nature Energy*** 2016, 2, 16191. |
| $Etched\text{-}NiOOH/BiVO_4$ | 5.43 | 200 h@0.8 $V_{RHE}$ | 1 M KBi+$Fe^{2+}$ | ***Angew. Chem. Int. Ed.*** 2020, 59, 6213. |
| $NiFeO_x/BiVO_4$ | 5.54 | 100 h@1.23 $V_{RHE}$ | 1 M KBi | ***Adv. Mater.*** 2020, 2001385. |
| NiOOH/NiOOH/2-$BiVO_4$ dual electrode | 5.87 | 100 h@1.23 $V_{RHE}$ | 1 M KBi | ***Adv. Mater.*** 2018, 30, 1800486. |
| NiOOH/black $P/BiVO_4$ | 4.48 | 60 h@1.23 $V_{RHE}$ | 0.5 M KPi | ***Nature Commun.*** 2019, 10, 2001. |
| $NiOOH/FeOOH/BiVO_4$ | 4.2 | 48 h@0.6 $V_{RHE}$ | 0.5 M KPi | ***Science*** 2014, 343, 990. |
| NiFeY $LDH/BiVO_4$ | 5.2 | 24 h@0.8 $V_{RHE}$ | 1 M KBi | ***ACS Catal.*** 2020, 10, 10570. |
| $Fh/BiVO_4$ | 4.78 | 50 h@0.61 $V_{RHE}$ | 0.4 M KBi | ***ACS Catal.*** 2017, 7, 1868. |
| NiOOH/FeOOH/ $TiO_{2-x}/BiVO_4$ | 6.12 | 100 h@1.23 $V_{RHE}$ | 0.5 M KPi | ***Adv. Energy Mater.*** 2019, 9, 1901287. |
| Molecular $Co_4O_4/BiVO_4$ | 5.0 | 140 s@0.7 $V_{RHE}$ | 0.5 KBi | ***Angew. Chem. Int. Ed.*** 2017, 56, 6911. |

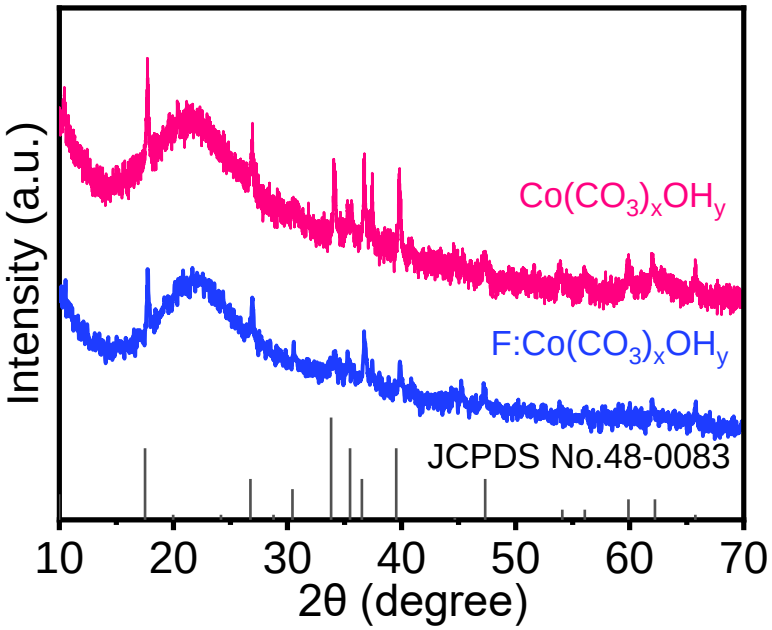


**Figure S1.** XRD patterns of $Co(CO_3)_xOH_y$ and $F:Co(CO_3)_xOH_y$. The powders of samples were collected from the bottom of autoclaves.

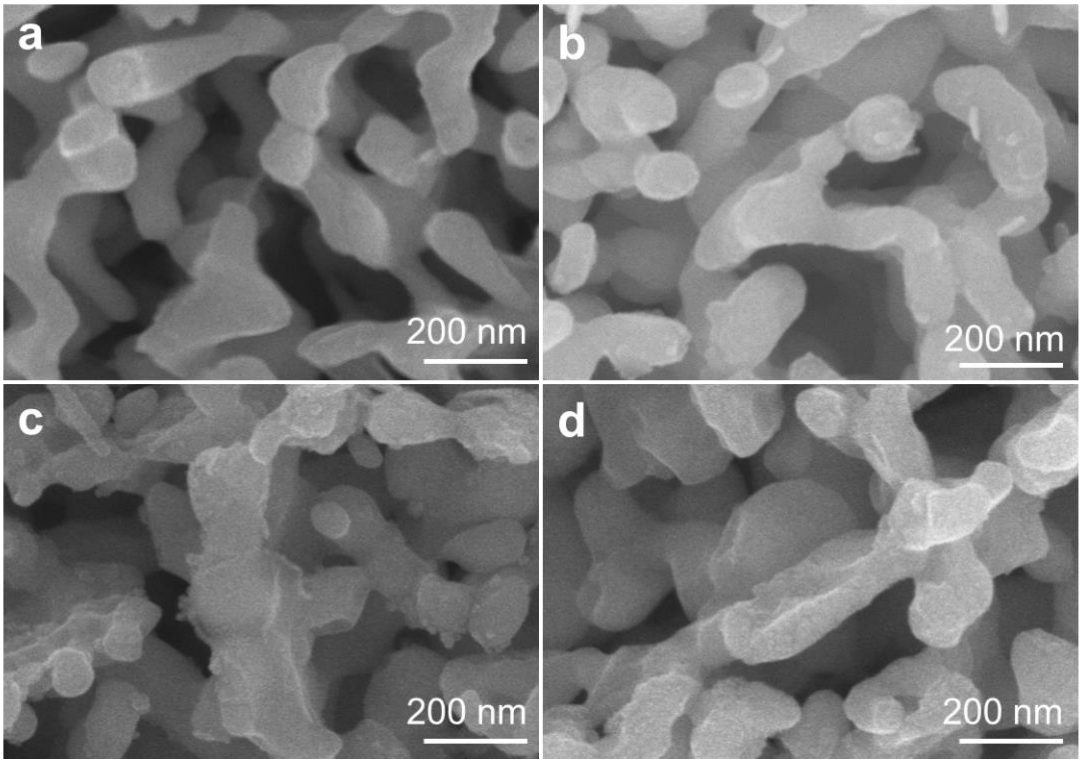


**Figure S2.** (a-d) SEM images of (a,c) $Co(CO_3)_xOH_y$/BVO and (b,d) F:$Co(CO_3)_xOH_y$/BVO (a,b) before and (c,d) after *J-t* measurement.

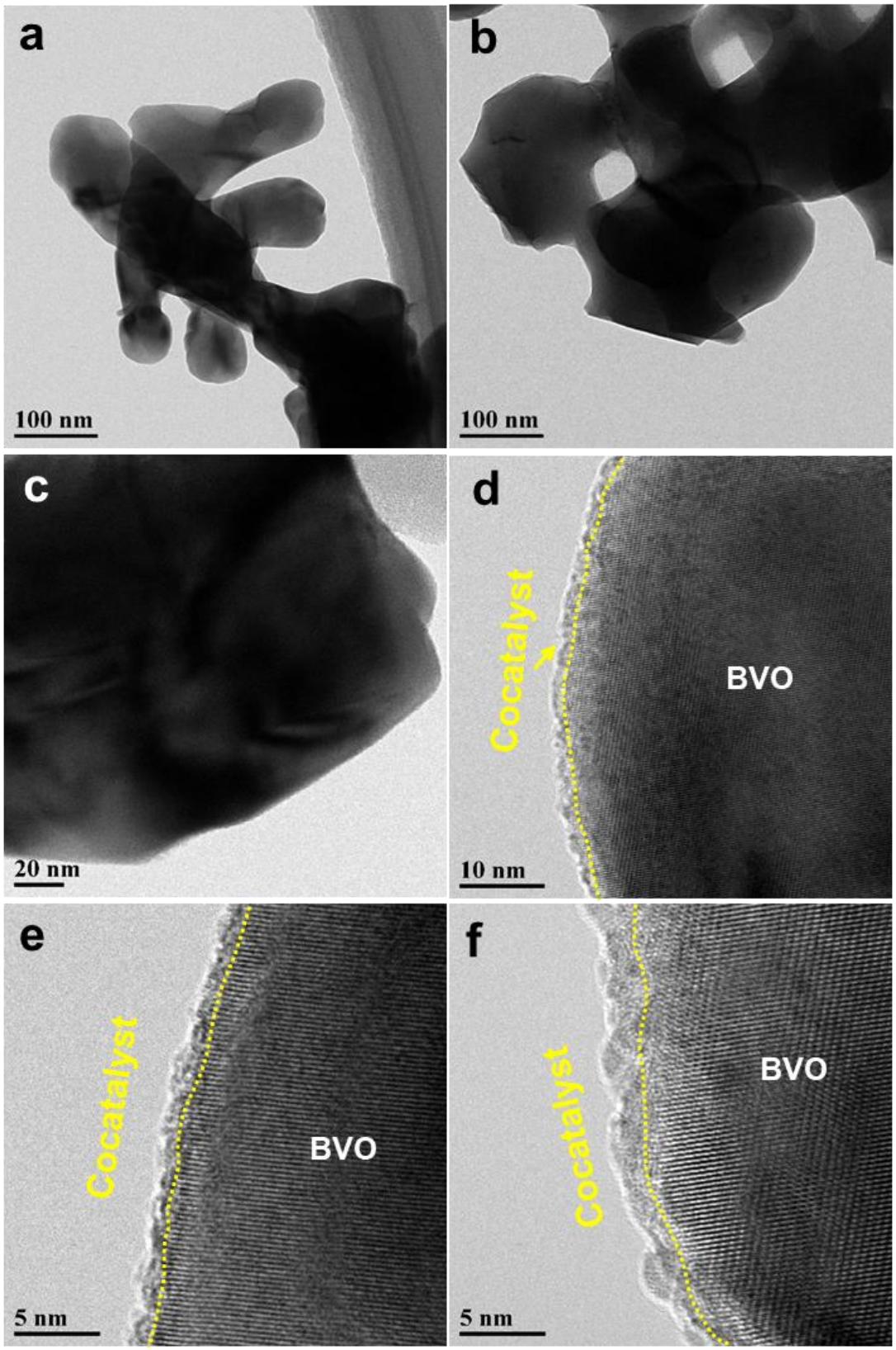


**Figure S3.** (a-d) TEM images of $Co(CO_3)_xOH_y$/BVO.

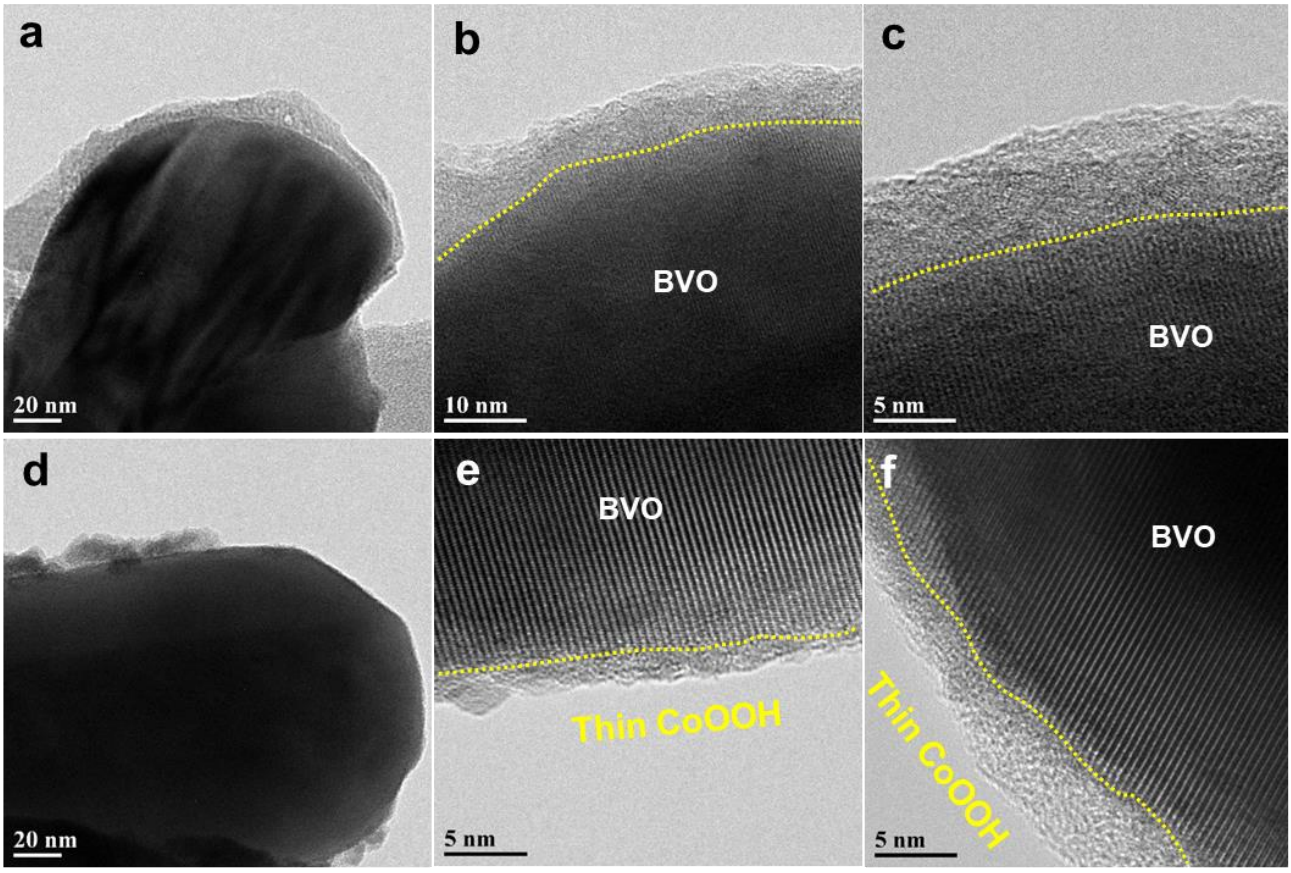


**Figure S4.** (a-f) TEM images of F:Co$(CO_3)_xOH_y$/BVO (a-c) before and (d-f) after *J-t* measurement.

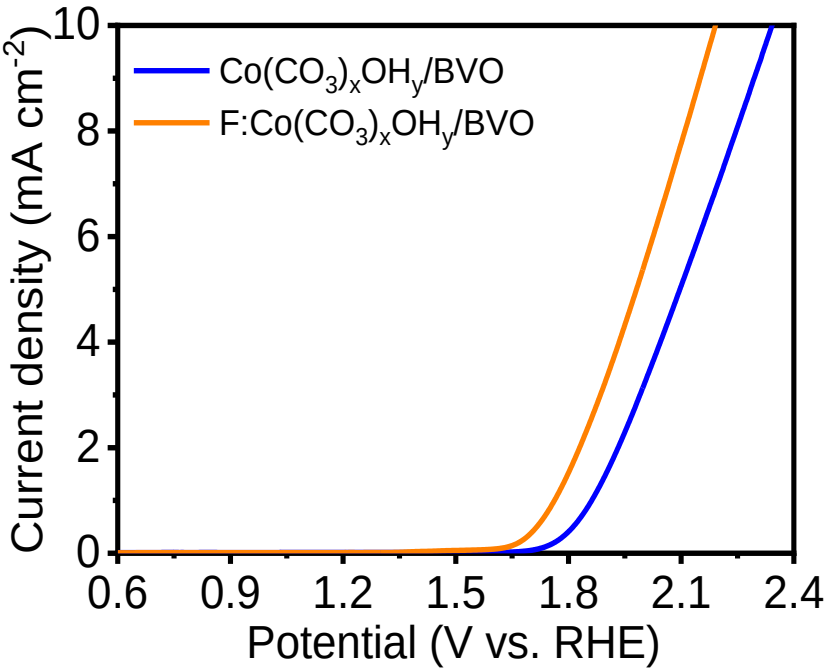


**Figure S5.** *J-V* curves of $Co(CO_3)_xOH_y$/BVO and F:$Co(CO_3)_xOH_y$/BVO in KBi under dark.

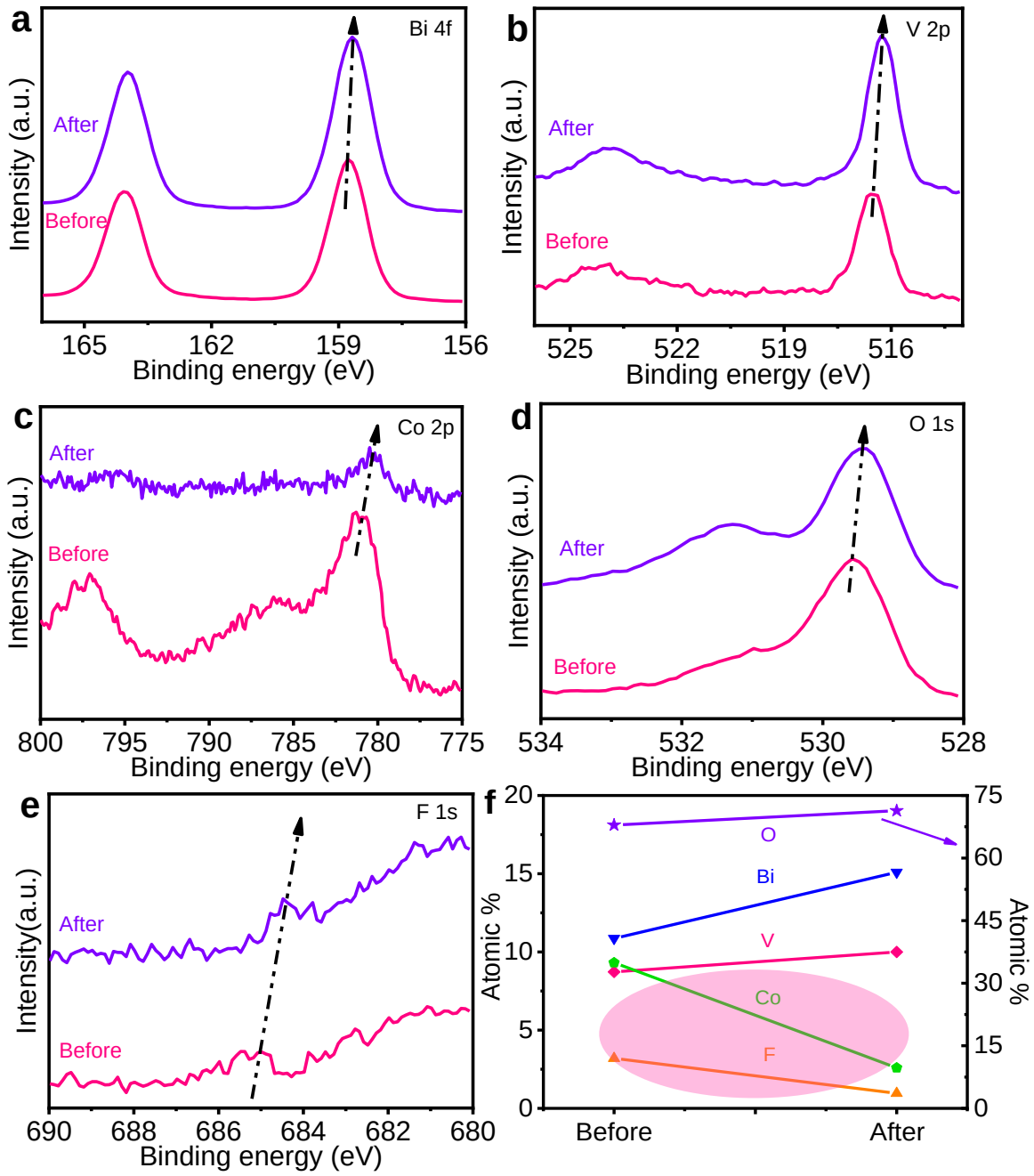


**Figure S6.** (a-d) XPS (a) Bi 4f, (b) V 2p, (c) Co 2p, (d) O 1s, and (e) F 1s spectra of F:Co$(CO_3)_xOH_y$/BVO before and after *J-t* meaurement of 20 h in KBi under AM 1.5G illumination; (f) element contents of corresponding electrodes.

The F 1s shows a main peak at 685 eV, and the peak intensity of F 1s is decreased after *J-t* meaurement, accompanying with a shift towards the lower B.E. (**Figure S6e**).

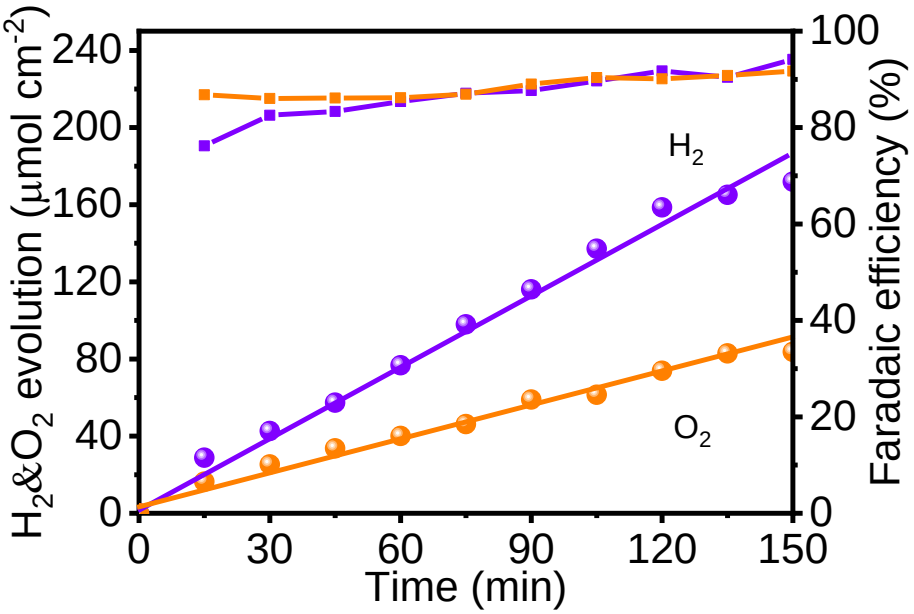


**Figure S7.** Oxygen and hydrogen evolution produced by gas chromatography and faradaic efficiency of $Co(CO_3)_xOH_y$/BVO at 1.23 $V_{RHE}$ for 5 h under AM 1.5G illumination in 1 M KBi+F.

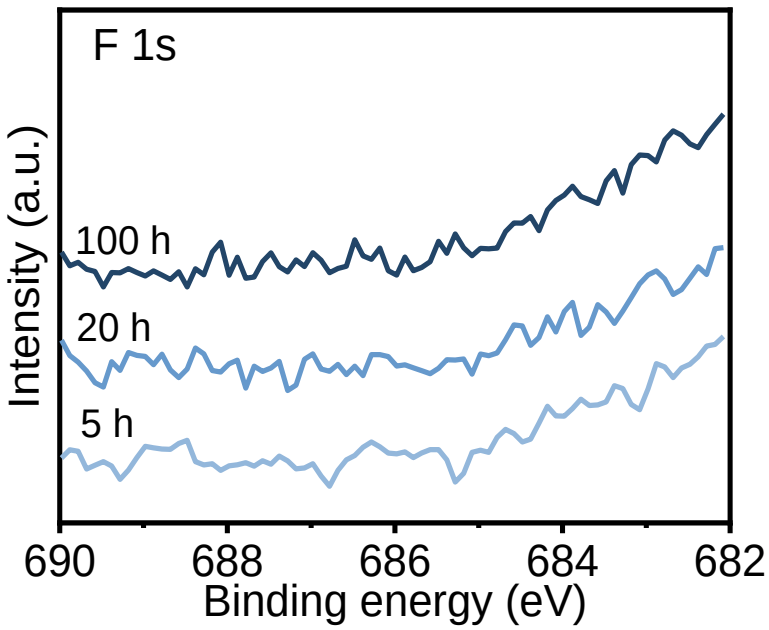


**Figure S8**. F 1s XPS spectra of $Co(CO_3)_xOH_y$/BVO in KBi+F at 0.6 $V_{RHE}$ for various times.

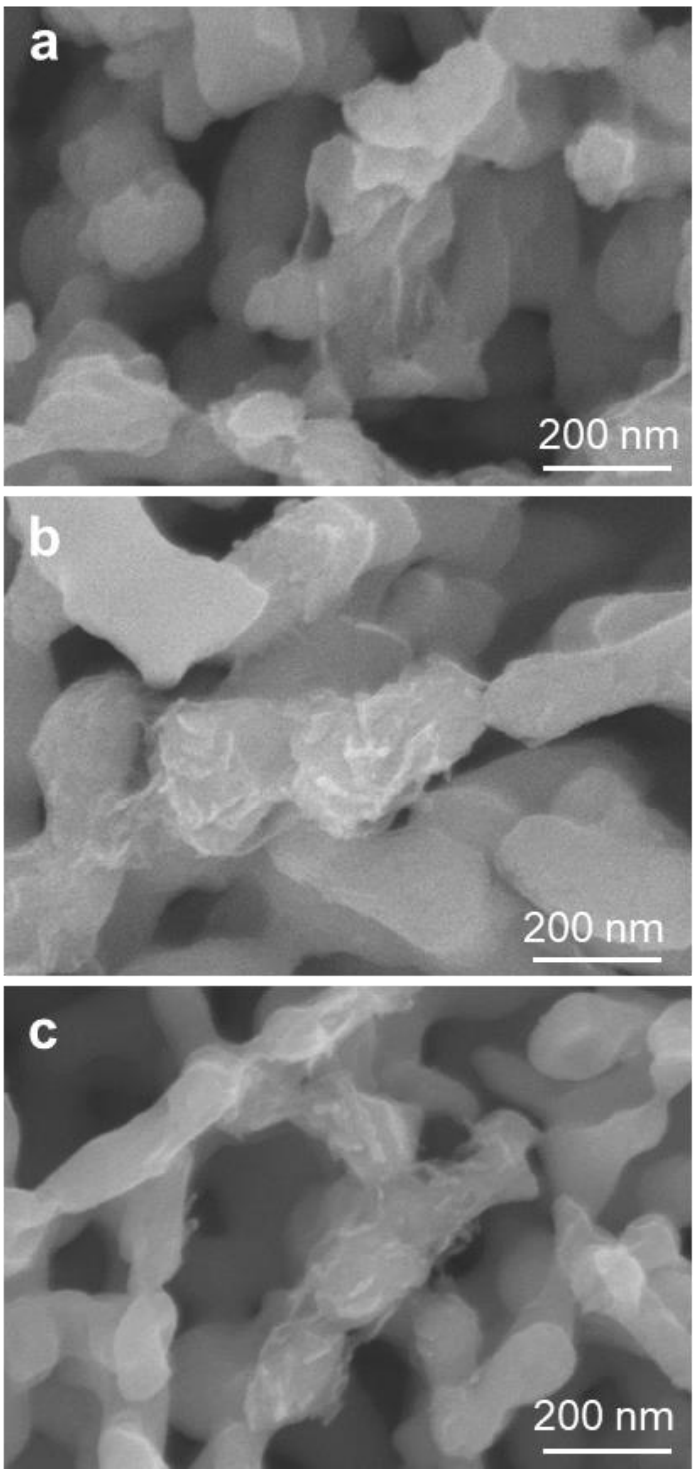


**Figure S9.** (a-c) SEM images of $Co(CO_3)_xOH_y$/BVO in (a) KBi+Co, (b) KBi+Fe, and (c) KBi+Ni electrolytes after *J-t* measurements for 1-3 h.

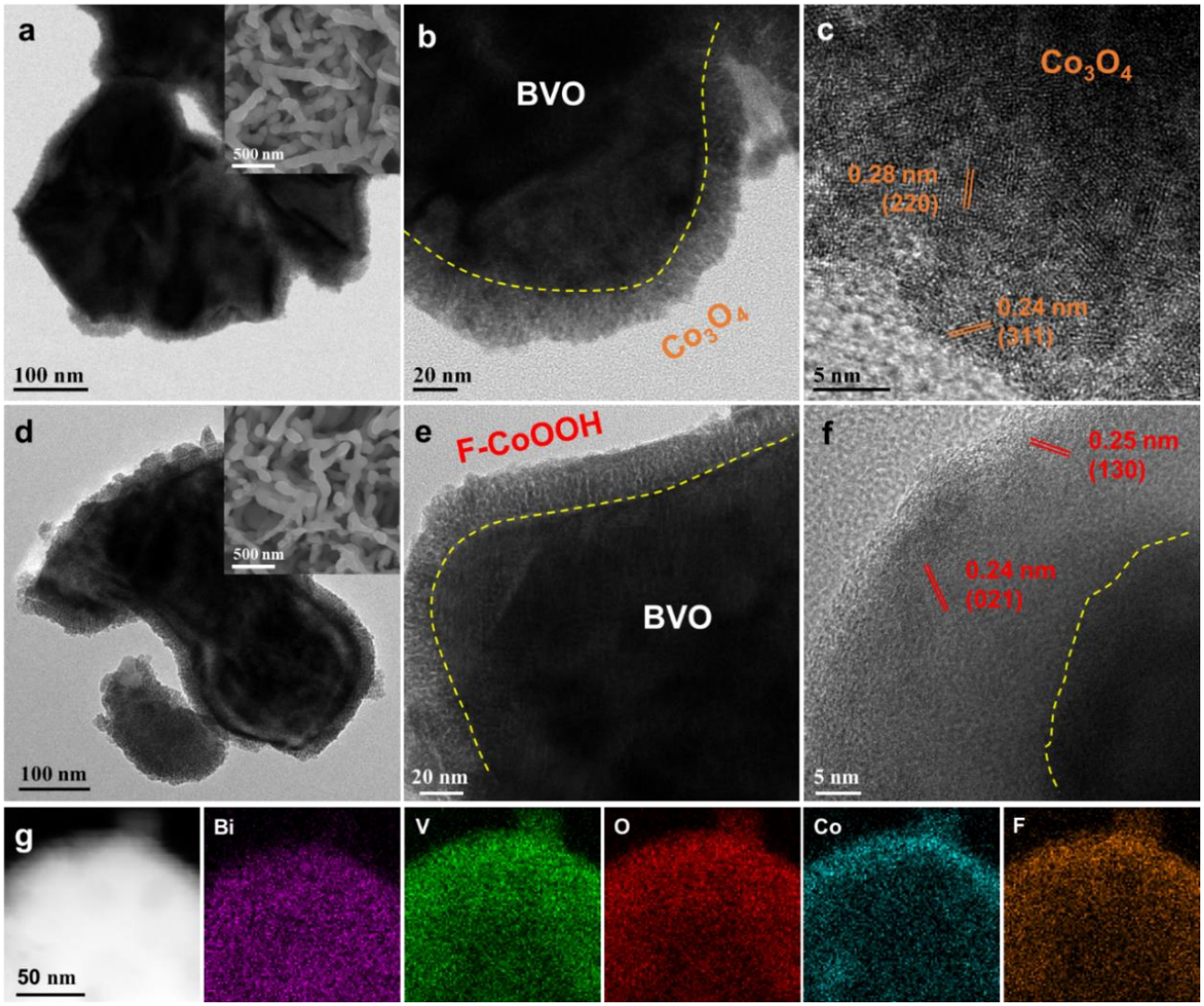


**Figure S10.** (a-c) TEM images of as-prepared $Co_3O_4$/BVO; (d-f) TEM images of activated $Co_3O_4$/BVO after *J-t* measurement in KBi+F; (g) TEM-EDS mapping of activated $Co_3O_4$/BVO after *J-t* measurement. The activated $Co_3O_4$/BVO was performed under *J-V* test for scanning in KBi+F.

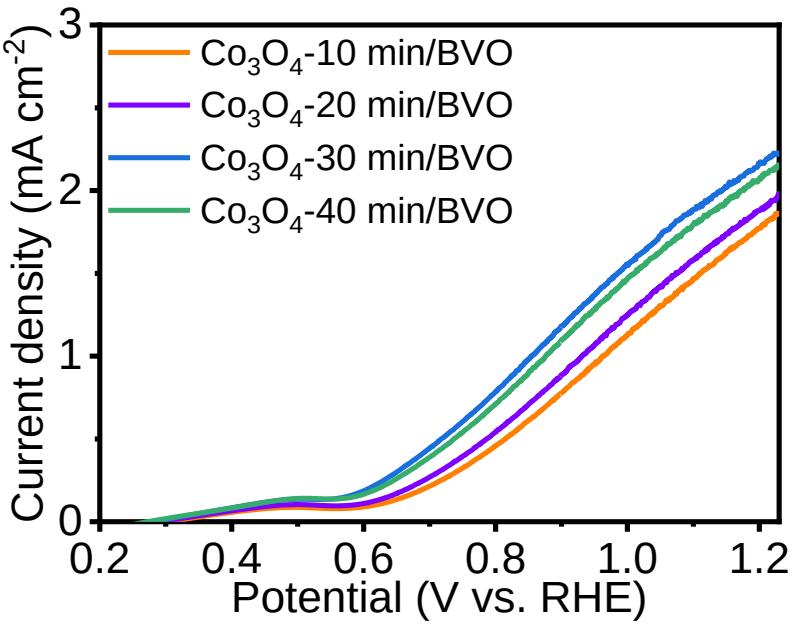


**Figure S11.** *J-V* curves of $Co_3O_4$/BVO electrodes with various hydrothermal times in KBi under AM 1.5G illumination.

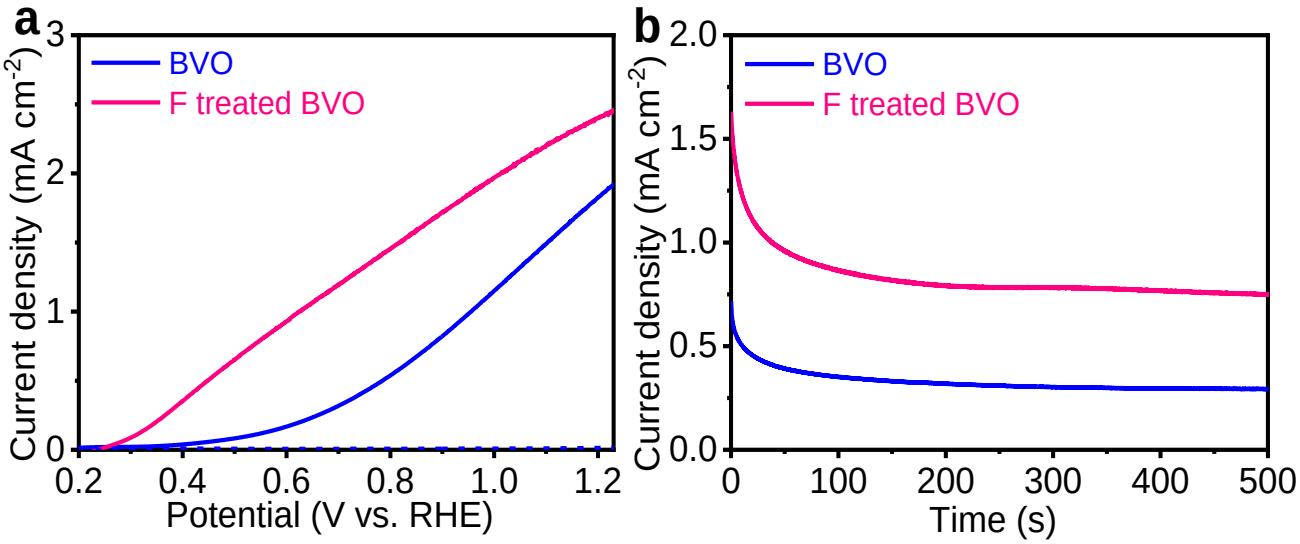


**Figure S12.** (a) *J-V* curves of BVO and F treated BVO in KBi under AM 1.5G illumination; (b) *J-t* curves of BVO and F treated BVO in KBi at 0.8 $V_{RHE}$ under AM 1.5G illumination. The BVO was treated in 1 M $NH_4F$ for 3 h (noted as F treated BVO).

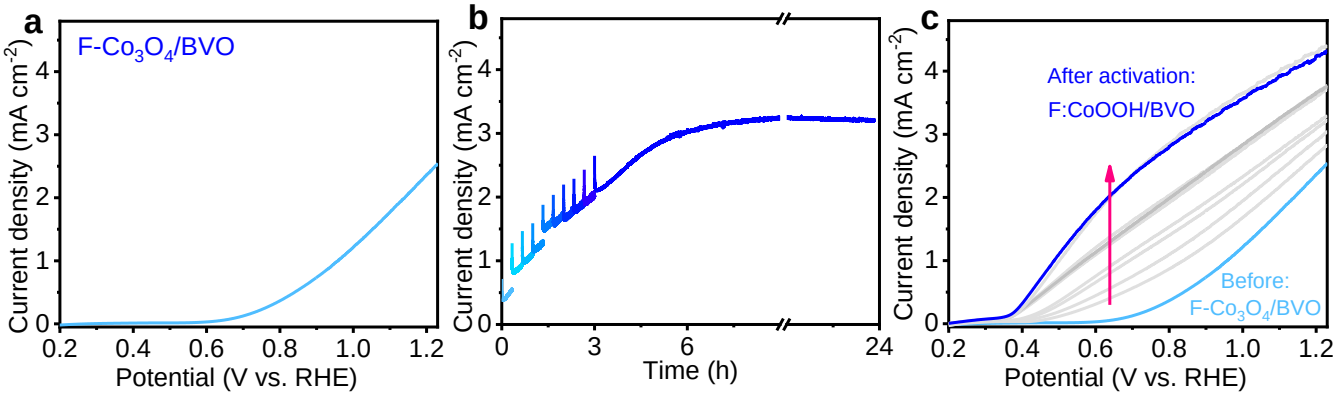


**Figure S13.** (a) *J-V* curve of F-$Co_3O_4$/BVO in 1 M KBi; (b) *J-t* plots of correspond sample at 0.8 $V_{RHE}$ for activation. The content of $NH_4F$ powder was controlled of 0.05 g; (c) *J-V* curves of F-$Co_3O_4$/BVO in KBi with various scanning cycles according to *J-t* measurement. All measurements were tested under AM 1.5G illumination.

For comparison, the F doped $Co_3O_4$ cocatalyst after thermal treatment was synthesized. The *J-V* curve of F-$Co_3O_4$/BVO electrode shows a low photocurrent in KBi (**Figure S13a**). The electrode was then applied a bias at 0.8 $V_{RHE}$ at a certain intervals under AM 1.5G illumination. The *J-t* curve (**Figure S13b**) exhibits that the photocurrent is initially decreased rapidly, and then rises gradually, accompanying with the improved *J-V* curve as illustrated in **Figure S13c**. The photocurrent reaches up to a maximum of 4.1 mA $cm^{-2}$ at 1.23 $V_{RHE}$, with a negative shift of onset potential from 0.65 $V_{RHE}$ (initial cycle) to 0.38 $V_{RHE}$. Further TEM examination (**Figure S14**) confirms that after the stability measurement, the cocatalyst layer becomes thinner 5~10 nm in thickness in contrast to the as-prepared electrode with a cocatalyst layer of 20~30 nm. This is consistent with the result of F:$Co(CO_3)_xOH_y$/BVO after *J-t* test, which is due to the transformation from F-$Co_3O_4$ to F:CoOOH during *J-t* measurement. The dissolution of cocatalyst is confirmed by XPS data (**Figure S15**), in which Co is reduced from 7.7 at.% to 6.48 at.%, accompanying with the loss of F from 4.76 at.% to 2.8 at.%.

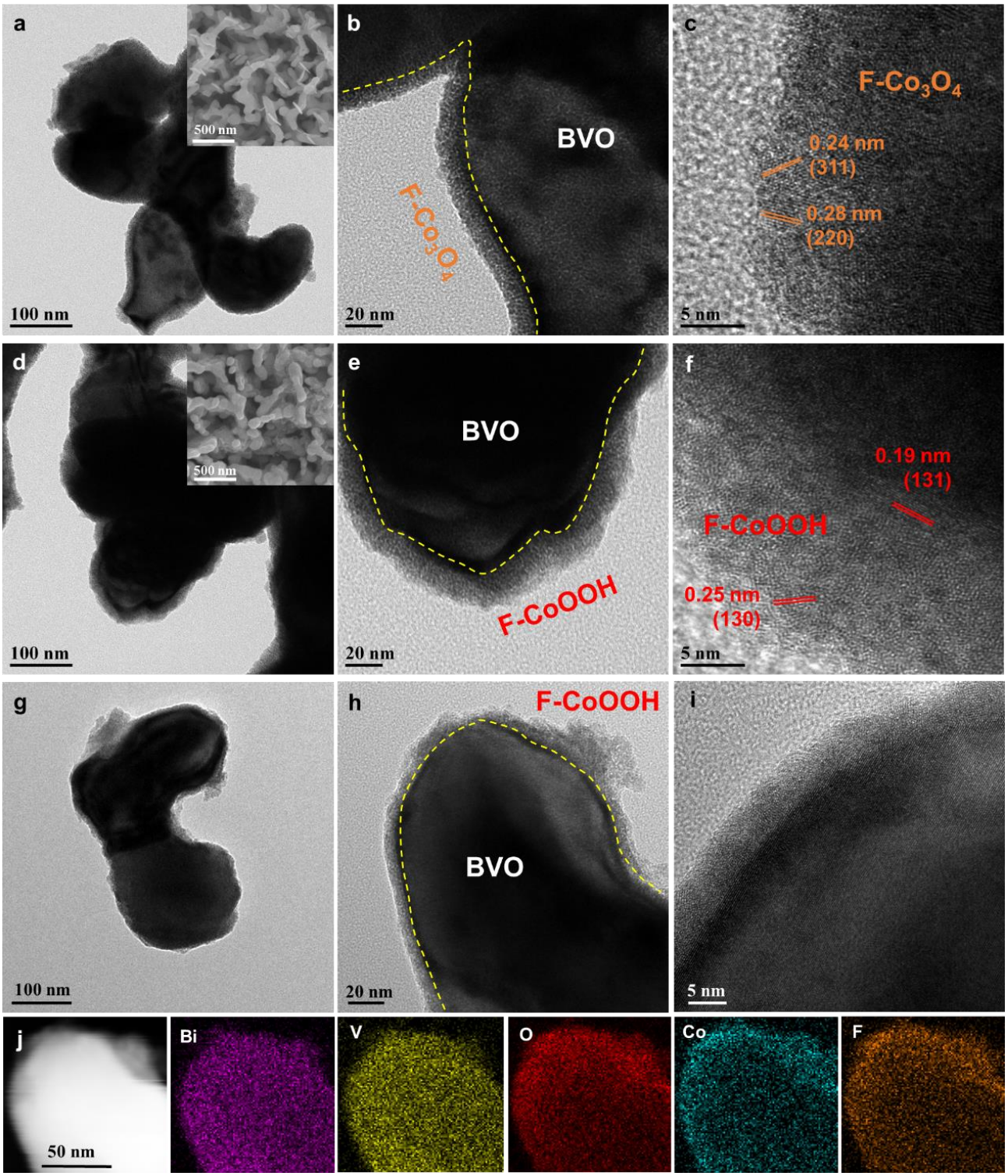


**Figure S14.** (a-c) TEM images of as-prepared F-$Co_3O_4$/BVO; (d-f) TEM images of activated F-$Co_3O_4$/BVO in KBi; (g-i) TEM images of activated F-$Co_3O_4$/BVO after *J-t* measurement; (j) TEM-EDS mapping of activated F-$Co_3O_4$/BVO after *J-t* measurement. The activated F-$Co_3O_4$/BVO was performed in KBi under *J-t* test with various scans.

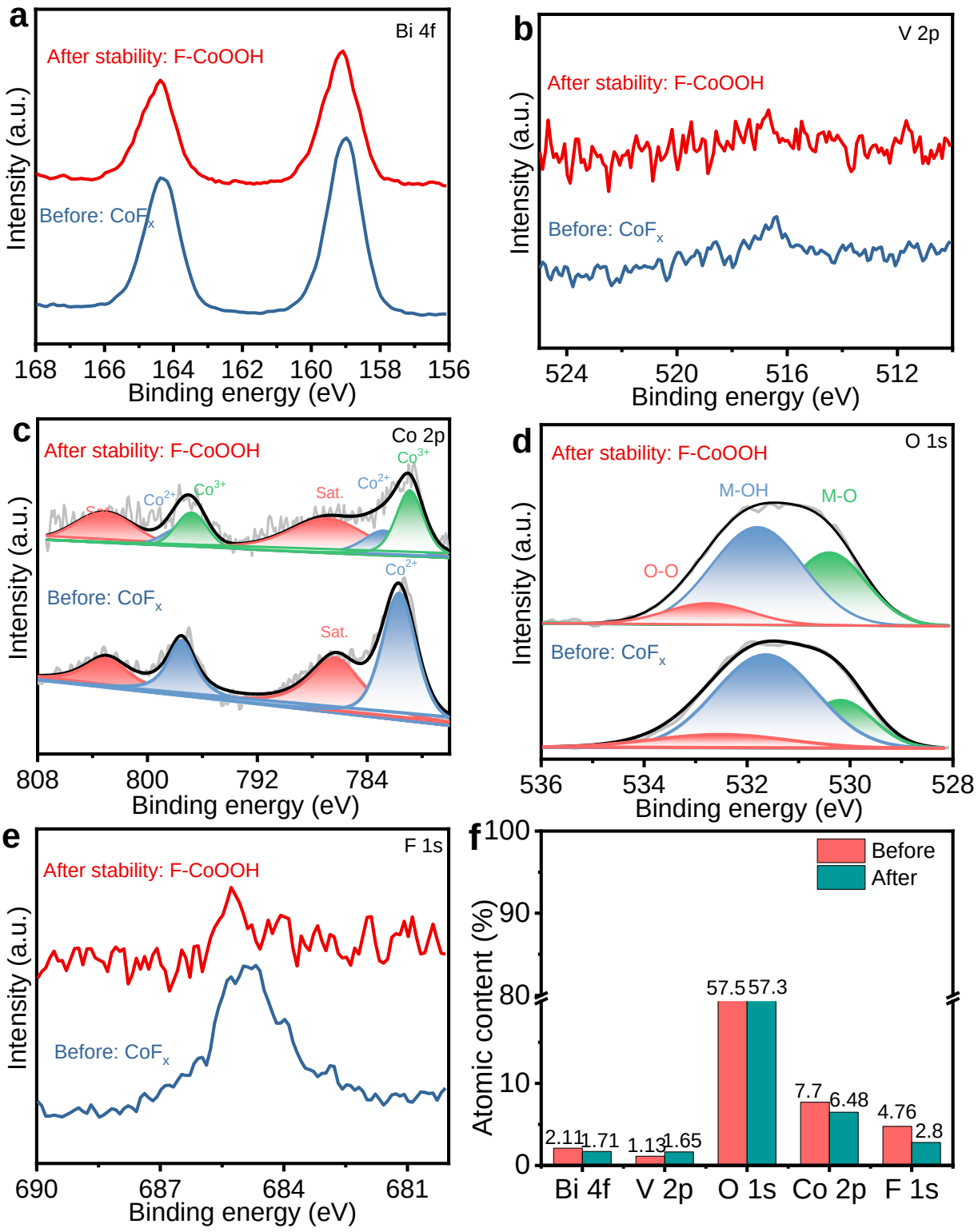


**Figure S15.** (a) Bi 4f, (b) V 2p, (c) Co 2p, (d) O 1s, (f) F 1s XPS spectra of F-$Co_3O_4$/BVO before and after activation; (f) atomic ratio of corresponding samples.

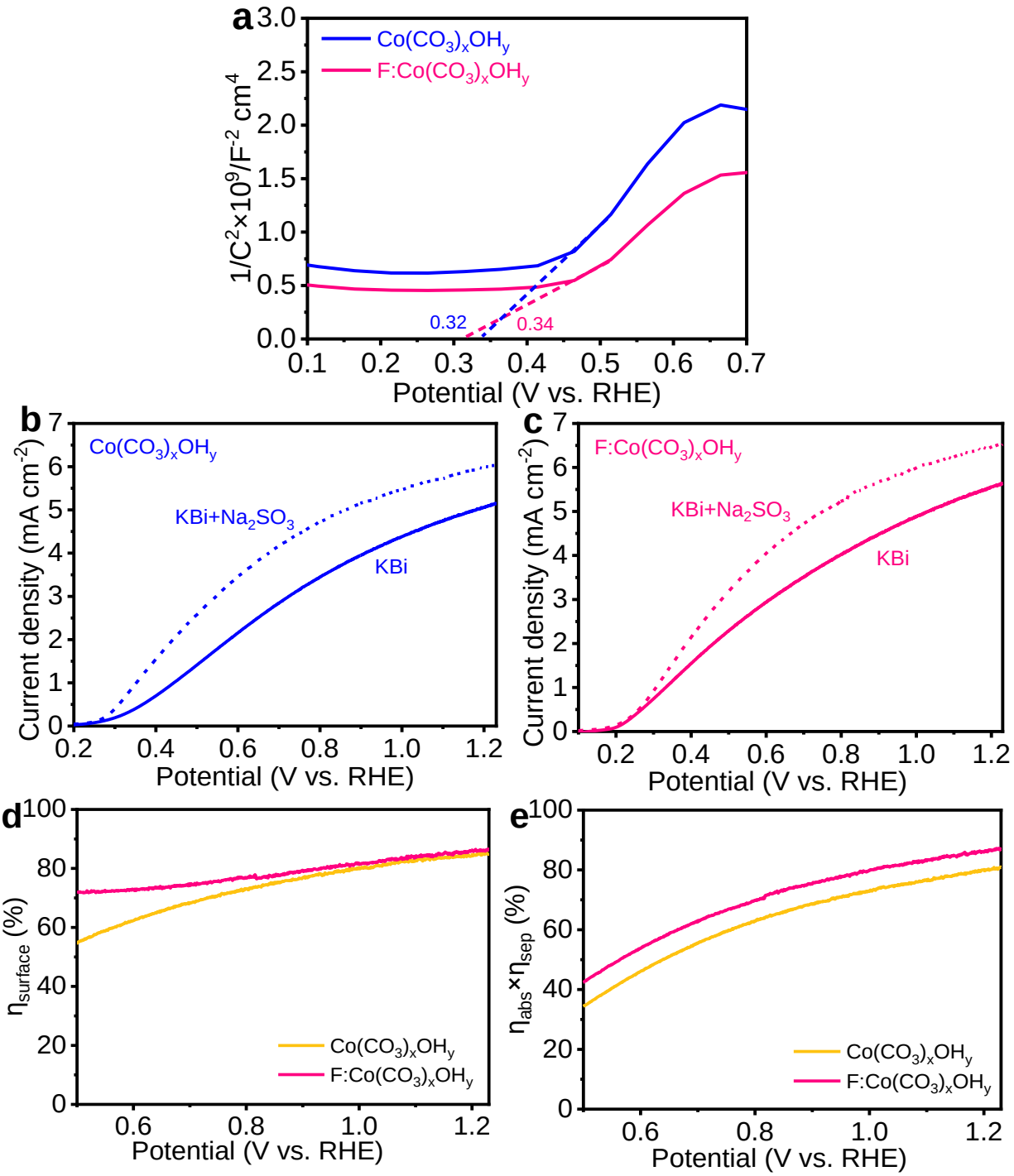


**Figure S16.** (a) Mott-Schottky measurements of $Co(CO_3)_xOH_y$/BVO and F:$Co(CO_3)_xOH_y$/BVO in KBi; (b) *J-V* curves of $Co(CO_3)_xOH_y$/BVO in KBi without and with $Na_2SO_3$; (c) *J-V* curves of F:$Co(CO_3)_xOH_y$/BVO in KBi without and with $Na_2SO_3$; (d) surface separation efficiency and (e) production of light absorption and charge separation of $Co(CO_3)_xOH_y$/BVO and F:$Co(CO_3)_xOH_y$/BVO.

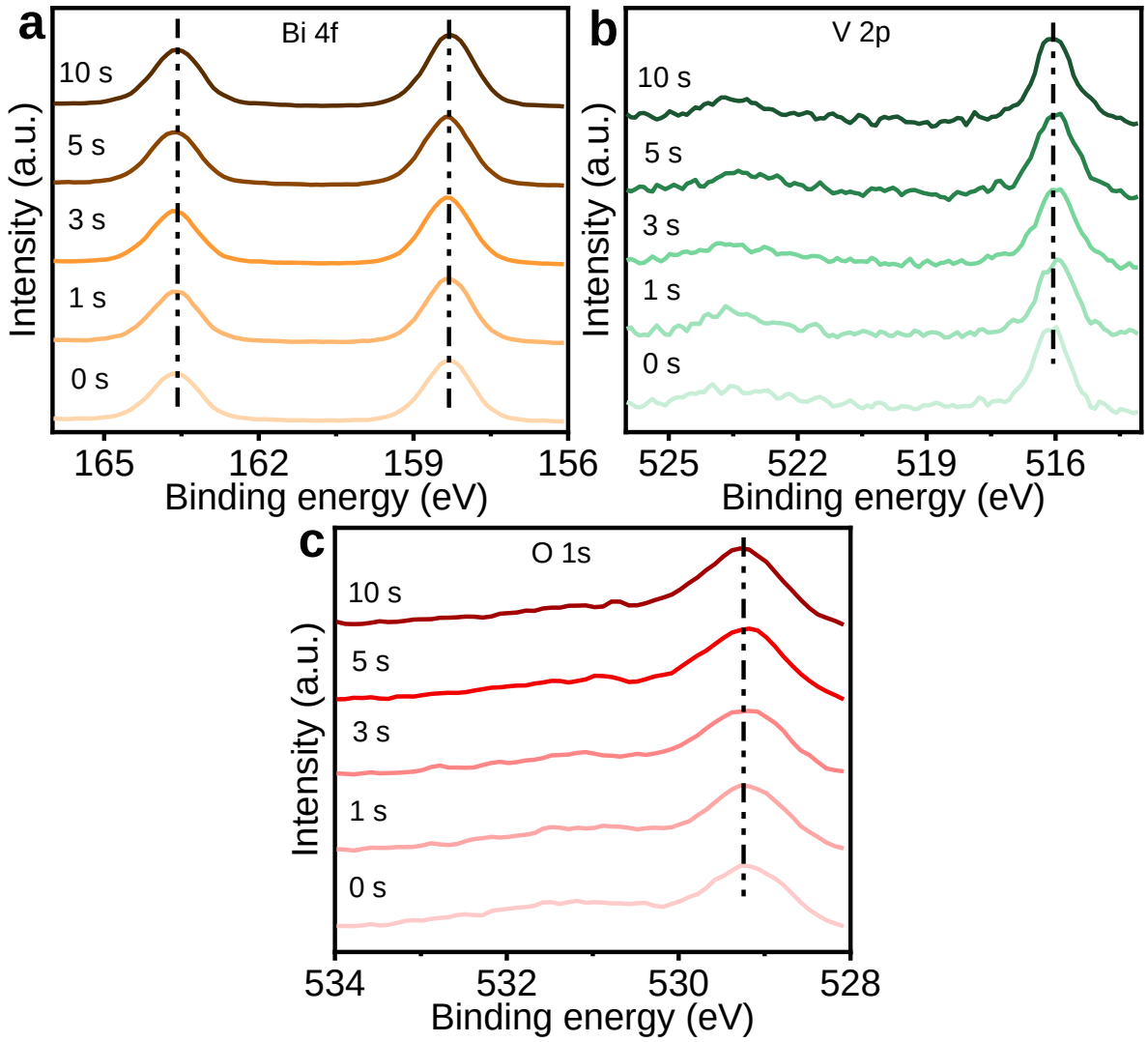


**Figure S17.** (a-c) XPS depth profiles of (a) Bi 4f, (b) V 2p, and (c) O 1s spectra of $Co(CO_3)_xOH_y$/BVO in KBi+F under *J-t* measurement at 0.6 $V_{RHE}$ for 2 h under AM 1.5G illumination.

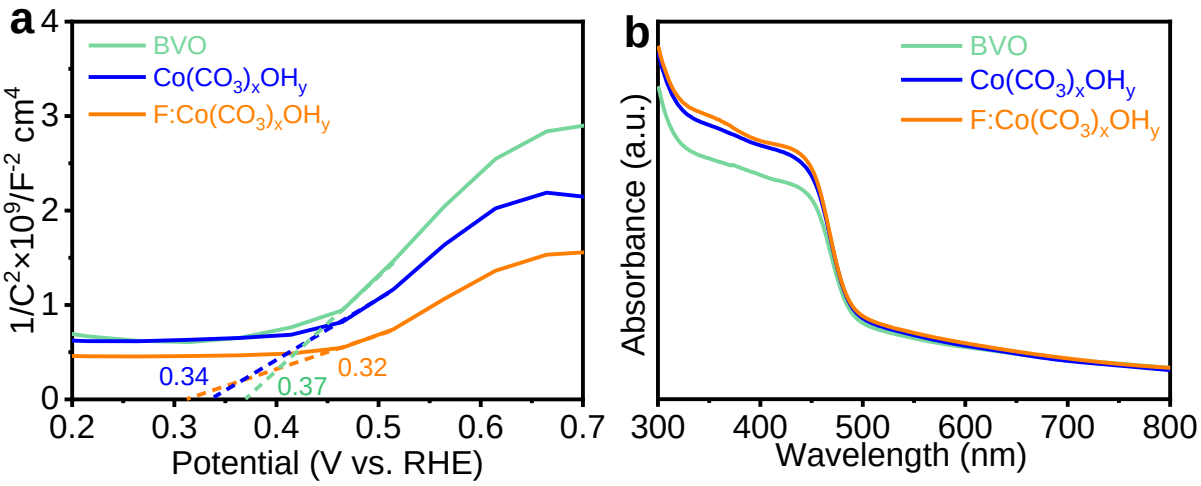


**Figure S18.** (a) Mott-Schottly plots and (b) UV-vis spectra of BVO, $Co(CO_3)_xOH_y$/BVO, and F:$Co(CO_3)_xOH_y$/BVO.

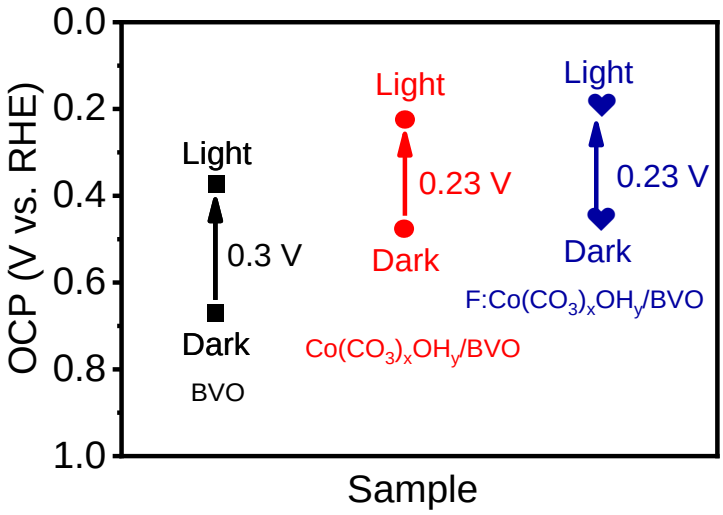


**Figure S19.** Open circuit potentials of BVO, $Co(CO_3)_xOH_y$/BVO, and F:$Co(CO_3)_xOH_y$/BVO electrodes.

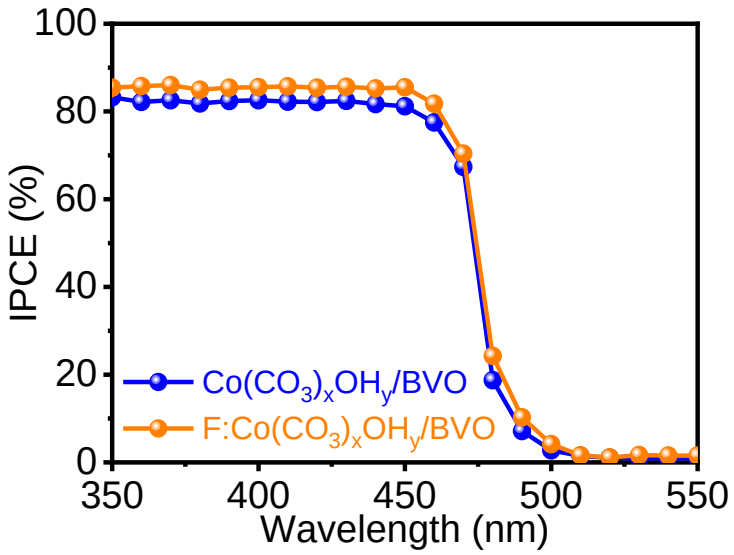


**Figure S20.** IPCE values of $Co(CO_3)_xOH_y$/BVO and F:$Co(CO_3)_xOH_y$/BVO electrodes.

**Table S2.** Comparison of IPCE values and charge efficiency for $BiVO_4$-based photoelectrodes.

| Photoanode | Electrolyte | $\eta_{trans}$ @1.23 $V_{RHE}$ | IPCE @1.23 $V_{RHE}$ | Reference |
|---|---|---|---|---|
| $Co(CO_3)_xOH_y/BiVO_4$ | 1 M KBi (pH=9.5) | 89% | 85%@430 nm | *J. Mater. Chem. A* 2020, 8, 2563. |
| Co-Pi/$BiVO_4$ | 0.5 M KPi (pH=7) | 71% | 70%@450 nm | *Energy Envrion. Sci.* 2018, 11, 1*299.* |
| Co-Pi/$BiVO_4$/ZnO | 0.3 M $Na_2SO_4$+KPi (pH=7.5) | --- | 40%@400 nm | *Nano Energy* 2017, 32, 232. |
| Co-Pi/$BiVO_4$ /Ta:$TiO_2$ | 0.5 M KPi (pH=7) | --- | 50%@450 nm | *ACS Cent. Sci.* 2016, 2, 80. |
| Co-Pi/$BiVO_4$ | 0.1 M KPi (pH=7) | --- | 70%@450 nm | *ChemSusChem* 2012, 5, 1420. |
| Co-Pi/$BiVO_4$/$WO_3$ | 0.1 M KPi (pH=7) | 75% | 60%@350 nm | *ACS Appl. Mater. Interfaces* 2018, 11, 5623. |
| Co-Ci/H,Mo:$BiVO_4$ | 0.1 M KPi (pH 7.0) | 95% | 80%@450 nm | *ACS Nano* 2015, 9, 11820. |
| U-CoOOH/$BiVO_4$ | 0.2 M $Na_2SO_4$ (pH=7) | 89% | 76%@420 nm | *J. Mater. Chem. A* 2019, 7, 4415. |
| $Co_4O_4$/$BiVO_4$ | 0.5 M KBi (pH=9.3) | 90% | 93%@420 nm | *Angew. Chem. Int. Ed.* 2017, 56, 6911. |
| CoO*x*/$BiVO_4$ /$WO_3$/$SnO_2$ | 0.5 M KPi (pH=7) | 85% | 55%@450 nm | *ACS Appl. Mater. Interfaces* 2017, 9, 1479. |
| **$Co(CO_3)_xOH_y/BiVO_4$** | **1 M KBi without and with $F^-$ (pH=9.5)** | **85%** | **83%@450 nm** | ***This work.*** |